Role of Loc1p in assembly and reorganization of nuclear *ASH1* messenger ribonucleoprotein particles in yeast

Annika Niedner[a,b,1], Marisa Müller[a,b,1,2], Balaji T. Moorthy[c], Ralf-Peter Jansen[c], and Dierk Niessing[a,b,3]

[a]Group Intracellular Transport and RNA Biology, Institute of Structural Biology, Helmholtz Zentrum München–German Research Center for Environmental Health, 85764 Neuherberg, Germany; [b]Department of Biochemistry, Gene Center of the Ludwig-Maximilians University, 81377 Munich, Germany; and [c]Interfaculty Institute of Biochemistry, Eberhard-Karls-Universität Tübingen, 72076 Tübingen, Germany

Edited by James E. Dahlberg, University of Wisconsin Medical School, Madison, WI, and approved November 19, 2013 (received for review August 12, 2013)

Directional transport of mRNA is a universal feature in eukaryotes, requiring the assembly of motor-dependent RNA-transport particles. The cytoplasmic transport of mRNAs is preceded by the nuclear assembly of pre-messenger ribonucleoprotein particles (mRNPs). In budding yeast, the asymmetric synthesis of HO 1 (*ASH1*) pre-mRNP originates already cotranscriptionally and passes through the nucleolus before its nuclear export. The nucleolar localization of *ASH1* mRNA protein 1 (Loc1p) is required for efficient *ASH1* mRNA localization. Immunoprecipitation experiments have revealed that Loc1p forms cocomplexes with other components of the *ASH1* transport complex. However, it remains unclear how Loc1p is recruited into this mRNP and why Loc1p is important for *ASH1* mRNA localization. Here we demonstrate that Loc1p undergoes a direct and specific interaction with the *ASH1* mRNA-binding Swi5p-dependent HO expression protein 2 (She2p). This cocomplex shows higher affinity and specificity for RNA bearing localization elements than the individual proteins. It also stabilizes the otherwise transient binding of She2p to *ASH1* mRNA, suggesting that cooperative mRNA binding of Loc1p with She2p is the required nuclear function of Loc1p for *ASH1* mRNA localization. After nuclear export, myosin-bound She3p joins the *ASH1* mRNP to form a highly specific cocomplex with She2p and *ASH1* mRNA. Because Loc1p is found only in the nucleus, it must be removed from the complex directly before or after export. In vitro and in vivo experiments indicate that the synergistic interaction of She2p and She3p displaces Loc1p from the *ASH1* complex, allowing free Loc1p to rapidly reenter the nucle(ol)us. Together these findings suggest an ordered process of nuclear assembly and reorganization for the maturation of localizing *ASH1* mRNPs.

macromolecular complex | reconstitution experiments | Puf6p | cotranscriptional recruitment

Messenger RNA localization is a universal feature of eukaryotes (1–3). By complementing transcriptional control (4), it fulfills a variety of functions, including the establishment of cell polarity and specialization of subcellular regions. In recent years, the directional transport of asymmetric synthesis of HO 1 (*ASH1*) mRNA in budding yeast has emerged as a particularly well-suited model to study mechanistic principles of RNA localization. Here, comparably few proteins participate in the directional transport of *ASH1* mRNA and about 30 other transcripts (5, 6).

Chromatin-immunoprecipitaton experiments revealed that the dedicated RNA-binding Swi5p-dependent HO expression protein 2 (She2p) binds already cotranscriptionally to nascent *ASH1* mRNA (7, 8). Two additional RNA-binding proteins, pumilio-homology domain family protein 6 (Puf6p) and heterogeneous nuclear RNP K-like protein 1 (Khd1p), are also present in the nucleus, bind to *ASH1* mRNA, and act in the cytoplasm as translational repressors during *ASH1* transport (9–12). A fourth nuclear factor, termed localization of *ASH1* mRNA protein 1 (Loc1p), has been implicated in the assembly of nuclear pre-messenger ribonucleoprotein particles (mRNPs). Like Puf6p, Loc1p is a nuclear protein (13) with an enrichment in the nucleolus (14, 15) and participates in the assembly of the large ribosomal subunit (16–18).

The composition of the nuclear *ASH1* mRNP was previously analyzed by coimmunoprecipitation experiments. By using She2p as bait, Puf6p, Loc1p, and *ASH1* mRNA were copurified (11, 19). The translational inhibitor Khd1p, which interacts with the 5′ region of *ASH1* mRNA (12), was absent from such purifications (11, 20). These data suggest the formation of a nuclear mRNP consisting of *ASH1* mRNA, She2p, Loc1p, and Puf6p.

Genomic deletion of *LOC1*, similar to *PUF6* (9, 11), leads to less efficient *ASH1* mRNA localization (13). Although Loc1p does not shuttle between nucleus and cytoplasm (13), *loc1*Δ cells show an up-regulation of cytoplasmic *ASH1* mRNA translation (13, 21), indicating that this protein is required for translational repression during localization. *ASH1* mRNA contains four *cis*-acting localization elements, which are also termed zip-code elements. These elements are specifically recognized by the transport complex. In the 5′–3′ order of the *ASH1* mRNA the zip-code elements are termed E1, E2A, E2B, and E3. Puf6p- (11) and Loc1p-dependent translational repression (21) seems to be mediated only by the E3 zip-code element. Thus, Loc1p might be required to remodel the nuclear precomplex for the assembly of translational repressors at the E3 element.

Significance

Cytoplasmic mRNA localization is preceded by the formation of nuclear pre-mRNPs. To date the requirement of the nuclear mRNP assembly is not well understood. We used *ASH1* mRNA localization from budding yeast to understand the mechanisms of nuclear priming for cytoplasmic mRNA transport. We found that the nuclear factor Loc1p is required to stably and specifically tether the bona fide *ASH1* RNA-binding protein She2p to RNA in the nucleus, offering an explanation for the requirement of Loc1p for *ASH1* mRNA localization. Because Loc1p is not part of the cytoplasmic *ASH1* mRNP, it must be removed before mRNA transport. We show that the cytoplasmic transport factor She3p displaces Loc1p from the *ASH1* mRNP, allowing for the maturation of the localizing *ASH1* mRNP.

Author contributions: A.N., R.-P.J., and D.N. designed research; A.N., M.M., and B.T.M. performed research; A.N., B.T.M., R.-P.J., and D.N. contributed new reagents/analytic tools; A.N., M.M., B.T.M., R.-P.J., and D.N. analyzed data; and A.N. and D.N. wrote the paper.

The authors declare no conflict of interest.

This article is a PNAS Direct Submission.

[1]A.N. and M.M. contributed equally to this work.

[2]Present address: Adolf-Butenandt-Institute and Center for Integrated Protein Science, Ludwig-Maximilians University, 80336 Munich, Germany.

[3]To whom correspondence should be addressed. E-mail: niessing@helmholtz-muenchen.de.

This article contains supporting information online at www.pnas.org/lookup/suppl/doi:10.1073/pnas.1315289111/-/DCSupplemental.

In a point-mutated She2p that is unable to enter the nucleus, no Puf6p and very little Loc1p are found associated with *ASH1* mRNA (19). Thus, She2p appears to play an important role for the assembly and/or recruitment of the nuclear precomplex including Puf6p and Loc1p. Vice versa, preventing nuclear export of She2p with a temperature-sensitive *mex67-5* mutant results in accumulation of She2p and *ASH1* mRNA in the nucleolus (14). Together, these observations indicate that the nucle(ol)ar fate is an essential step for the assembly of mature, translationally silent *ASH1* mRNA-transport complexes.

ASH1 mRNA is exported into the cytoplasm along with She2p and Puf6p, whereas Loc1p remains located in the nucleolus (13, 14, 22). Once in the cytoplasm, the *ASH1* precomplex interacts with another subcomplex consisting of the type V myosin motor myosin 4 (Myo4p) and the RNA-binding protein She3p. The nuclear and cytoplasmic precomplexes form the mature transport complex via the direct interaction between She2p and She3p and their synergistic binding to the zip-code elements of the *ASH1* mRNA (8, 23–28).

Although Puf6p is associated with the localizing *ASH1* mRNP, in vitro binding studies suggested that Puf6p and She2p interact only indirectly via their joint binding to the *ASH1* mRNA (8). For Loc1p and She2p or for Loc1p and Puf6p no such information is available. It also remains unclear whether these factors depend on each other for RNA binding, whether they compete for *ASH1* mRNA interaction, and whether they all participate in the same mRNP or form different subcomplexes. Furthermore, no mechanism has been described that explains how Loc1p is removed from the complex prior to or during nuclear export.

Here we report the characterization of the nuclear *ASH1* mRNP assembly. We found that Loc1p and She2p directly and specifically interact with each other. This cocomplex of She2p and Loc1p shows a significantly better affinity, stability, and specificity toward *ASH1* mRNA. Because the RNA binding of She2p alone is very transient, this cooperative interaction of Loc1p and She2p with *ASH1* mRNA appears to be essential for stably tethering She2p to nuclear *ASH1* mRNA. We do not observe a similar recruitment of Puf6p to the mRNP by Loc1p, She2p, or She3p. Thus, the importance of both factors for Puf6p binding to *ASH1* mRNA is likely more indirect. Because Loc1p is absent in the cytoplasm, it has to be removed from the mRNP during complex maturation. We found that She3p outcompetes Loc1p from its cocomplex with She2p and RNA, which results in the synergistic cocomplex of She2p, She3p, and *ASH1* mRNA as well as free Loc1p. This outcompetition offers a mechanistic explanation for the removal of Loc1p from the mRNP. Consistently, genomic deletion of *SHE3* in vivo perturbs the nucleolar localization of Loc1p.

Results

Loc1p Binds Directly and Specifically to She2p. Loc1p was shown to copurify with She2p from yeast extracts (19). To test whether this interaction is direct, we performed pull-down experiments with recombinant maltose binding protein (MBP)-tagged Loc1p and She2p. To exclude indirect, RNA-mediated interactions, proteins were purified under stringent conditions and successful removal of nucleic acid contaminations was verified before binding experiments (*Materials and Methods*; for Loc1p, see Fig. S1*A*). She2p was retained on amylose resin in the presence of Loc1p but not with MBP alone or in the absence of an MBP-tagged protein (Fig. 1*A*). Thus, the pull-down experiments suggest a direct and quantitative interaction between Loc1p and She2p.

Loc1p is involved not only in mRNA localization but also in ribosome biogenesis. It has been proposed that the effect of Loc1p on *ASH1* mRNA localization might be only an indirect effect of impaired ribosome function (21). On the other hand, Loc1p has been found in complex with *ASH1* mRNA, She2p, and Puf6p (13, 19), suggesting a direct and functional link. We performed additional in vitro pull-down experiments in the absence of RNA and found that Loc1p interacts selectively with She2p, but not with Puf6p, His-tagged She3p (She3p-H6), or GST (Fig. 1 *A* and *B*). Thus, Loc1p binding to She2p is selective, which rather indicates a direct role of Loc1p in *ASH1* mRNA localization.

Loc1p and She2p Form a Joint Cocomplex on the E3 Zip-Code Element of the *ASH1* mRNA. Yeast three-hybrid experiments were used to identify Loc1p as an *ASH1* E1 and E3 zip-code–binding protein (13). Binding to the E3 zip-code element was further confirmed in electrophoretic mobility shift assays (EMSAs), using either yeast extracts or bacterial extracts with recombinant Loc1p. In EMSAs with purified Loc1p we show that this protein indeed binds directly to the E3 zip-code element (Fig. 1*C*). The appearance of a higher molecular weight band further indicates that a second binding event occurs at a higher protein concentration.

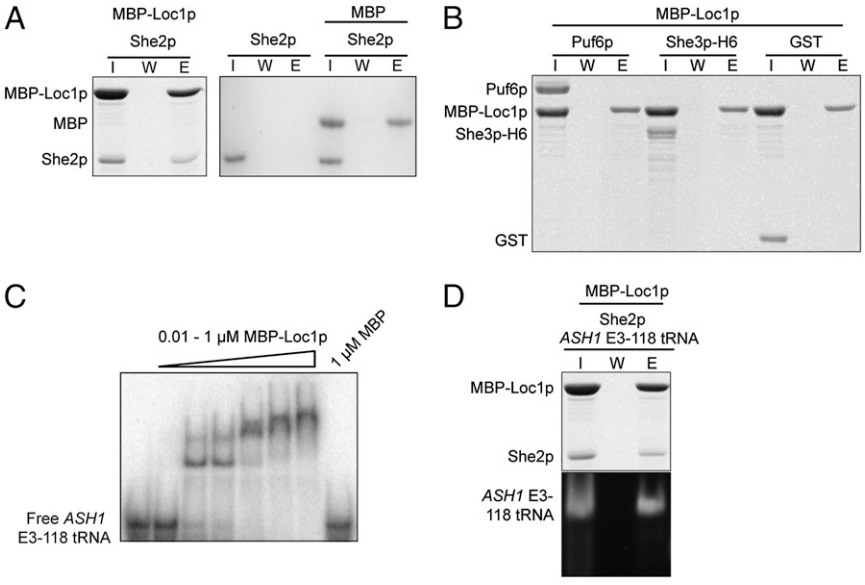

Fig. 1. Loc1p directly interacts with She2p and *ASH1* mRNA. (*A*) In pull-down experiments with amylose resin, MBP-Loc1p copurifies and thus directly interacts with recombinant She2p. Staining after SDS/PAGE was performed with Coomassie blue. (*B*) Pull-down experiments with MBP-Loc1p and Puf6p, She3p-H6, or GST. Loc1p is not able to pull down any of the tested proteins, indicating that this protein selectively interacts with She2p. Experimental setup is the same as in *A*. (*C*) EMSA with Loc1p and radioactively labeled E3 zip-code element of the *ASH1* mRNA reveals binding at nanomolar protein concentrations. (*D*) Amylose pull-down experiment with MBP-Loc1p, She2p, and the E3 element of *ASH1* mRNA suggests formation of a ternary complex. (*Upper*) Coomassie blue-stained SDS/PAGE; (*Lower*) agarose gel stained with GelRed.

Next, we asked whether the protein interaction between Loc1p and She2p is altered by binding to zip-code RNA. For better purification of large amounts of zip-code RNA, we used the tRNA-scaffold technique (29). We fused the 118-bases-long *ASH1* E3 element to a tRNA (*ASH1* E3-118 tRNA), expressed it in bacteria, and purified it. Using amylose resin and MBP-Loc1p, we pulled down She2p as well as *ASH1*-E3-118 tRNA (Fig. 1*D*), suggesting the formation of a ternary complex of these components.

Cooperative Binding of She2p and Loc1p to *ASH1* mRNA. The pull-down of She2p with RNA and Loc1p indicates a joint complex, but fails to yield direct information about their RNA binding within the complex. Furthermore, pull-down experiments are performed at micromolar concentrations that greatly exceed the nanomolar concentrations of these proteins in the cell. To directly assess RNA binding under more physiological conditions, we performed UV cross-linking experiments with radioactively labeled *ASH1* E3 RNA. Because UV cross-linking efficiency occurs preferentially with certain amino acids, such experiments yield semiquantitative information on affinities. As demonstrated before (8), at a concentration of 250 nM, She2p alone showed a well-detectable cross-linking product (Fig. 2*A*, lane 3). Also Loc1p alone could be cross-linked to the RNA (Fig. 2*A*, lanes 4–6). However, this cross-linking gave a clearly detectable signal only at 1 μM protein concentration. The combination of Loc1p and She2p led to a strong increase of the Loc1p–RNA cross-link (Fig. 2*A*, lanes 7–9). This observation indicates that She2p is required for efficient recruitment of Loc1p to *ASH1* mRNA. Because the She2p cross-link also showed an increased intensity in the presence of Loc1p, these results suggest cooperativity in RNA binding.

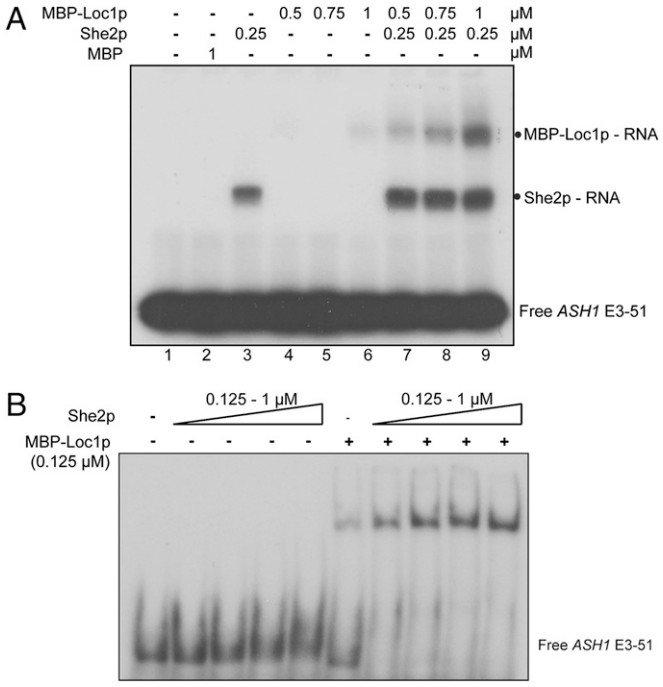

Fig. 2. She2p and Loc1p recruit each other to the *ASH1* mRNA. (*A*) UV cross-linking experiments with MBP-Loc1p, She2p, and radioactively labeled *ASH1* E3-51 RNA. In the presence of She2p and Loc1p, cross-linking of both proteins to the *ASH1* mRNA is increased (lanes 7–9). Note that in UV cross-linking experiments the used concentrations better reflect the physiological range than in pull-down experiments. (*B*) EMSA with She2p, MBP-Loc1p, and radioactively labeled *ASH1* E3-51 RNA. As observed before (8, 30), nanomolar concentrations of She2p do not lead to the formation of a significant band shift. This and complementing observations suggested a rather transient binding mode of She2p to the *ASH1* E3 RNA. In contrast, Loc1p shows a weak but detectable band shift at 125 nM concentration. When She2p is added with increasing concentrations, the observed band shift is considerably strengthened, indicating a cooperative binding event.

To validate these observations with a more quantitative assay, we performed EMSAs with constant, low concentrations of MBP-Loc1p and increasing concentrations of She2p (Fig. 2*B*). As previously shown (8, 30), in our EMSAs She2p alone does not form a protein–RNA complex stable enough to yield a significant mobility shift even at 1 μM She2p concentration (Fig. 2*B*). In contrast, Loc1p alone gives rise to a distinct band shift at a concentration of 125 nM. When both proteins are combined, a much stronger band shift was observed (Fig. 2*B*). Supershift experiments with increasing antibody concentrations further confirmed that She2p was indeed present in this shifted band (Fig. S2*A*, *Left*). Mobility shift assays with gradient gels that better separate larger complexes show the additional slow-migrating band expected for the ternary complex of She2p, Loc1p, and RNA (Fig. S2*A*, *Right*). These findings, together with the UV cross-linking experiments, indicate a cooperative recruitment of She2p and Loc1p onto the *ASH1* mRNA and a stabilization of She2p on the RNA by Loc1p.

Cocomplex of Loc1p and She2p Forms Only with Zip-Code RNA. Next, we wanted to assess the specificity of the ternary complex formed by She2p, Loc1p, and RNA for the *ASH1* E3 zip-code element. First, we performed pull-down experiments with glutathione resin and GST-tagged She2p as bait. In these experiments with *ASH1* E3-51 RNA and tRNA competitor but in the absence of Loc1p, we observed copurification of *ASH1* E3-51 RNA but not of the tRNA competitor (Fig. 3*A*). Addition of Loc1p resulted in the pull-down of *ASH1* E3-51 RNA and Loc1p, but not of tRNA competitor. Interestingly, in the experiment with She2p and Loc1p, a higher molecular weight band was observed in the urea PAGE (Fig. 3*A*, asterisk). Because this band disappeared after phenol-chloroform extraction (Fig. 3*A*, *Right*), the ternary complex of She2p, Loc1p, and *ASH1* E3-51 RNA was likely not completely disrupted by the presence of urea in the gel. Such a high molecular weight band was not observed in absence of Loc1p (Fig. 3*A*, *Left*).

When we repeated these pull-down experiments with the HIV TAR-57 tRNA as an unspecific, zip-code–lacking control instead of an *ASH1* zip-code RNA, we failed to observe copurification of Loc1p or RNA (Fig. 3*B*). Because She2p and Loc1p undergo a direct protein–protein interaction in the absence of RNA (Fig. 1*A*), this result suggests different binding modes of this complex for specific and unspecific RNAs. The disruption of the protein–protein interaction between She2p and Loc1p in the presence of HIV TAR-57 RNA (Fig. 3*B*) suggests competitive binding events, instead of the previously observed cooperative binding of She2p and Loc1p to zip-code RNA (Figs. 1*D* and 2 *A* and *B*). Consistent with this interpretation is the observation that in an amylose-resin pull-down, MBP-Loc1p copurified She2p only in the presence of zip-code–containing RNAs (Fig. S2*B*).

To confirm this difference in specific and unspecific RNA-binding modes by a different approach, we performed again UV cross-linking experiments. Radioactively labeled *ASH1* E3-51 tRNA efficiently cross-linked with She2p, Loc1p, and as a positive control She3p (Fig. 3*C*). Also in the cocomplex, Loc1p and She2p both efficiently cross-linked with the zip-code–containing RNA, as observed before (Fig. 2*A*). In contrast, the control HIV TAR-57 tRNA failed to show major cross-linking bands with She2p, Loc1p, or their cocomplex. Only She3p, which served as a control for unspecific binding (8), showed a clear cross-link (Fig. 3*C*). Also in competition experiments we observed a preference for *ASH1* E3 zip-code element (Fig. S2*C*). In summary,

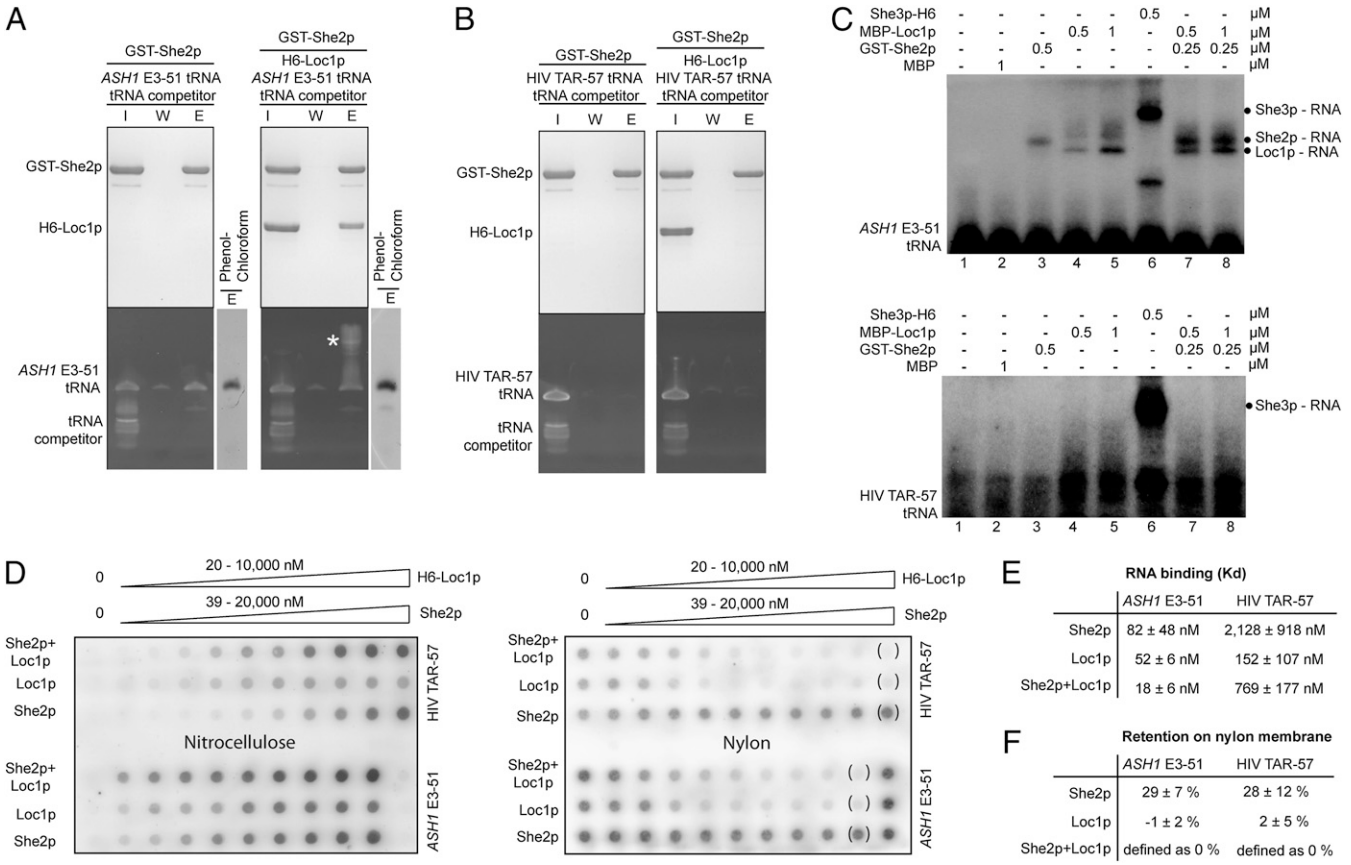

Fig. 3. The cocomplex of Loc1p and She2p mediates specific and stable binding to zip-code RNA. (*A*) In pull-down assays with glutathione Sepharose, GST-She2p copurifies *ASH1* E3-51 tRNA and H6-Loc1p. *Upper* gel shows PAGE and *Lower* gel shows an urea PAGE. The pull-down of *ASH1* E3-51 tRNA with GST-She2p and Loc1p showed an RNA species migrating at higher molecular weight (open asterisk). This species disappeared only after phenol-chloroform extraction (*Lower Right* gel), indicating the presence of stable ternary complexes in the urea gel. (*B*) Pull-down assays as in *A* but with the control HIV TAR-57 tRNA showed no copurification of Loc1p or RNA. In contrast to *ASH1* E3-51 tRNA, no ternary complex is formed and Loc1p appears to outcompete the unspecific RNA binding of She2p. Pull-down experiments with Loc1p as bait gave similar results (Fig. S2*B*). (*C*) UV cross-linking experiments with radioactively labeled *ASH1* E3-51 tRNA (*Upper*) or HIV TAR-57 tRNA (*Lower*). Whereas *ASH1* E3-51 tRNA efficiently cross-linked with She2p, Loc1p, She3p, and the She2p-Loc1p cocomplex, HIV TAR-57 tRNA cross-linked only with She3p. (*D*) Representative images of nitrocellulose (*Left*, RNA–protein complexes) and nylon (*Right*, free RNA) membranes from filter-binding assays with *ASH1* E3-51 tRNA or HIV TAR-57 tRNA. (*E*) Table summarizing the equilibrium dissociation constants (K_d) of three independent filter-binding experiments (*D*). The determined K_d value of Loc1p is in good agreement with EMSA in Fig. 1*C* and the K_ds for She2p with *ASH1* E3-51 and HIV TAR-57 RNA are consistent with previous quantifications (8, 30, 37). (*F*) Table showing the percentage of radioactively labeled RNA bound to the nylon membrane at saturated protein concentrations (marked with parentheses on nylon membrane in *D*). RNA bound to the nylon membrane represents the fraction of RNA that was not bound by protein and therefore was not retained on the nitrocellulose membrane. Because the She2p-Loc1p cocomplex interacts very stably with RNA and yields almost no signal on the nylon membrane, we defined these conditions as 0% retention. A stronger retention of RNA on the nylon membrane with She2p confirms its previously reported low complex stability. Values with ± show SD from three independent experiments.

these experiments suggest a clear preference in binding for the *ASH1* E3-51 RNA over the control RNA.

Cocomplex of She2p and Loc1p Shows Selectively Increased Affinity and Stability for Zip-Code RNA. For a quantitative assessment of the observed difference in RNA binding, we performed double-filter–binding experiments (31). In these experiments, a nitrocellulose membrane retains protein-bound radioactively labeled RNA, whereas a second nylon membrane retains free, unbound RNA. We used the radioactivity retained on the first membrane to determine equilibrium dissociation constants (K_d) and radioactivity on the second, nylon membrane to estimate the fraction of unbound RNA. Because filter-binding assays involve washing steps after initial binding, the latter can be used to assess complex stabilities.

Binding of the She2p-Loc1p cocomplex to *ASH1* E3-51 RNA showed an improved affinity (K_d = 18 nM) compared with that of the individual proteins (K_d for She2p = 82 nM and for Loc1p = 52 nM; Fig. 3 *D* and *E* and Fig. S3). The cocomplex of She2p and Loc1p had an over 40-fold lower affinity for the HIV TAR-57 tRNA (K_d = 769 nM). Interestingly, the She2p-Loc1p cocomplex had a 5-fold lower K_d for the control RNA compared with Loc1p alone (769 nM vs. 152 nM; Fig. 3 *D* and *E* and Fig. S3). The opposite effect was observed in binding experiments with the *ASH1* RNA (18 nM vs. 52 nM; Fig. 3 *D* and *E* and Fig. S3), further supporting the notion that the modes of binding for zip-code–containing and unspecific RNAs might be different.

Also the amounts of protein-free RNA retained on the nylon membrane indicated a difference in binding. The cocomplex of Loc1p and She2p as well as Loc1p alone retained almost no free RNA on the nylon membrane, indicating that the vast majority of RNA was stably associated with the protein-bound fraction at the nitrocellulose membrane (Fig. 3*D*). In contrast, She2p alone was unable to retain a comparable amount of RNA on the first membrane (Fig. 3*D*). These results indicate that the interaction of She2p with

RNA is stabilized by Loc1p. This stabilization effect was quantified by comparing signal intensities on the nylon membrane with the stable ternary complex of Loc1p, She2p, and RNA defined as 0% retention. Whereas we did not observe a difference in complex stability between Loc1p alone and the ternary complex, She2p showed a larger fraction of free RNA bound to the nylon membrane (Fig. 3*F*). The latter confirms the previously described (8, 30) low complex stability of the She2p–RNA interaction.

In Pull-Down Experiments Loc1p and She2p but Not Loc1p and Puf6p Form a Cocomplex with RNA. Like Loc1p, Puf6p coimmunoprecipitates with She2p and *ASH1* mRNA from yeast extracts (19) and localizes to the nucleolus (14, 15). However, in pull-down experiments Loc1p and Puf6p fail to interact (Fig. 1*B*). To study Puf6p interactions in the presence of RNA we used the E3-118 zip-code element, which contains two conserved Puf6p binding sites (see Table S3) (11). Initially we tested whether Puf6p can be pulled down by MBP-Loc1p or H6-Loc1p in the presence of *ASH1* E3-118 RNA. As before, we ensured that both proteins reproducibly showed monodisperse behavior in size-exclusion chromatography and normal RNA-binding capacity (Fig. 1*C* and Fig. S1 *B* and *C*). Puf6p was not retained by MBP-Loc1p on amylose beads (Fig. 4*A*), although Puf6p alone efficiently binds to E3 RNA (Fig. S1*C*) (8). Even by using pull-down conditions more closely resembling a physiological situation (250 nM protein) and different Loc1p and Puf6p tags, we were not able to detect an interaction between Loc1p and Puf6p (Fig. S4 *A* and *B*). Amylose pull-down experiments with MBP-Loc1p, She2p, Puf6p, and *ASH1* E3 mRNA showed similar results. All factors were retained on amylose resin, except for Puf6p (Fig. 4*B*). These data indicate that the proteins Loc1p and She2p form a stable cocomplex with *ASH1* mRNA, in which Puf6p does not participate.

UV Cross-Linking Reveals That Puf6p Is Not Recruited by Other Factors to the *ASH1* E3 Zip-Code RNA. To directly assess RNA-binding events at near-physiologic concentrations, we performed UV cross-linking experiments with radioactively labeled *ASH1* E3-118 RNA. Puf6p alone showed only a faint RNA cross-link (Fig. 4*C*, lane 4; for a longer exposure of this UV cross-link, see Fig. S4*D*). Also the presence of other proteins, such as She2p (Fig. S4*C*, lanes 7 and 8), She2p and She3p (Fig. 4*C*, lanes 6 and 7, and Fig. S4*D*), or She2p and Loc1p (Fig. 4*C*, lanes 8 and 9, and Fig. S4*D*) did not enhance the intensity of the Puf6p RNA cross-link. Vice versa, Puf6p did not alter the cross-linking of Loc1p, She2p, and She3p or combinations thereof. This indicates that Puf6p is not recruited by any of these factors to the *ASH1* E3 zip-code RNA.

The Cocomplex of She2p and She3p Displaces Loc1p from the RNA. She2p and *ASH1* mRNA, but not Loc1p mRNA, is exported into the cytoplasm (13, 22). Therefore, a mechanism must be in place that allows Loc1p to be removed from the mRNA before or during its export into the cytoplasm. Because Loc1p contains multiple potential nuclear-localization signals (Fig. S5), one mechanism could be that a strong nuclear reimport of Loc1p is sufficient to strip off this protein from the RNA. Alternatively, Loc1p could be actively displaced from the RNA by another component of the transport complex that joins the mRNP during or after nuclear export. A potential candidate for such

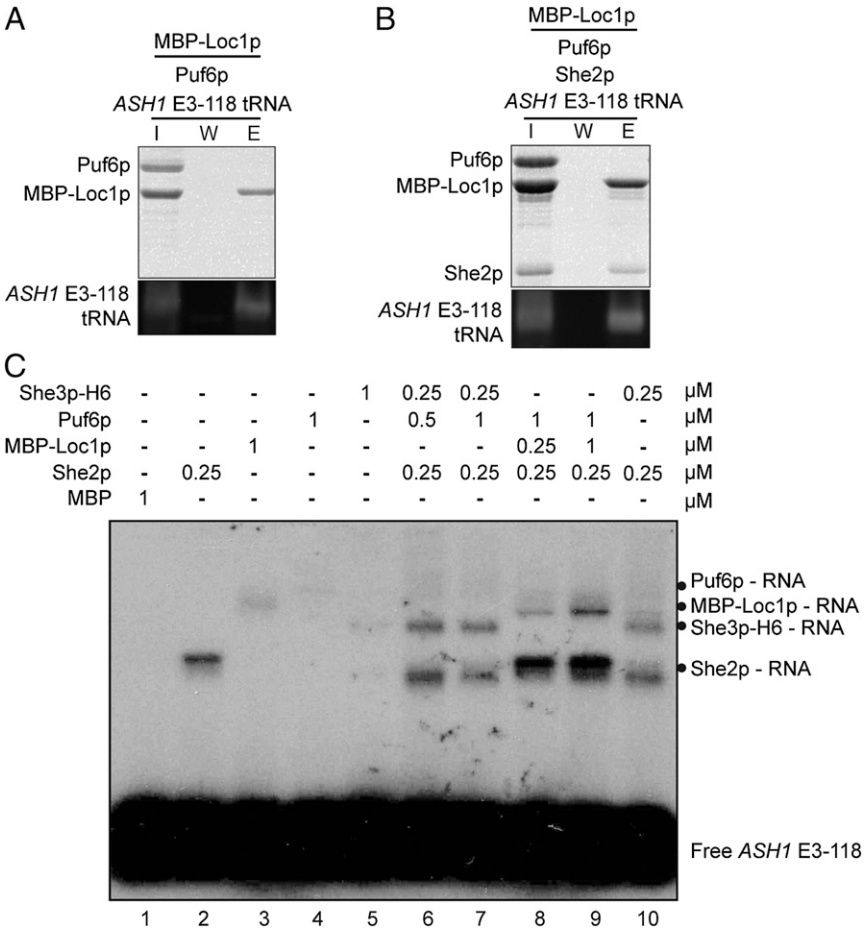

Fig. 4. Puf6p does not join the ternary complex of Loc1p, She2p, and RNA. (*A*) Pull-down experiment with amylose resin and MBP-Loc1p shows that Puf6p does not form a cocomplex with Loc1p and RNA. (*B*) Pull-down experiment with MBP-Loc1p, She2p, Puf6p, and the *ASH1* E3 zip-code RNA. All components except for Puf6p can be pulled down as a cocomplex. Experimental setup is as shown in Fig. 1. (*C*) UV cross-linking experiments with radioactively labeled *ASH1* E3-118 RNA and She2p, MBP-Loc1p, She3p-H6 and Puf6p. The presence of She2p and She3p-H6 (lanes 6 and 7) or She2p and MBP-Loc1p (lanes 8 and 9) does not increase the intensity of the Puf6p–RNA cross-link, indicating the absence of a recruitment mechanism for Puf6p. A longer exposure of this cross-link is depicted in Fig. S4*D*.

an active displacement is the myosin adapter and RNA-binding protein She3p. In the cytoplasm, it forms a high-affinity cocomplex with She2p and *ASH1* mRNA. Also Loc1p binds to both She2p (Fig. 1*A*) and *ASH1* mRNA (Figs. 1 *C* and *D* and 2). Thus, for an active displacement, She3p would need to outcompete Loc1p from both binding partners.

We first tested whether the addition of She3p to Loc1p, She2p, and *ASH1* E3 element changes the association of Loc1p with the RNA. To detect RNA-binding events at near-physiologic concentrations, we used again UV cross-linking of radioactively labeled *ASH1* E3 zip-code RNA. Whereas we recapitulated the Loc1p recruitment to the *ASH1* RNA by She2p (Fig. 5*A*, compare lanes 3–5 with lanes 6 and 7), the combined presence of She2p and She3p almost completely abolished RNA cross-linking by Loc1p (Fig. 5*A*, lanes 8 and 9). This finding indicates that at nanomolar, near-physiological concentrations the She2p-She3p complex displaces Loc1p from zip-code–containing RNA.

Formation of the Ternary Complex of She2p, She3p, and *ASH1* RNA Disrupts the Interaction between She2p and Loc1p. This UV cross-linking experiment does not rule out the possibility that Loc1p remains directly bound to She2p, even when it is displaced from the RNA. Hence, we tested in pull-down experiments whether She3p alters the interaction of She2p and Loc1p in the absence and presence of RNA. Indeed, we found that MBP-Loc1p fails to interact with She2p and She3p in the absence of the E3 element (Fig. 5*B*). We also performed these experiments with the *ASH1* E3 element and an unspecific tRNA competitor. Also under these experimental conditions Loc1p was not able to pull down She2p or She3p (Fig. 5*C*). We conclude that She3p also outcompetes the protein interaction of Loc1p with She2p.

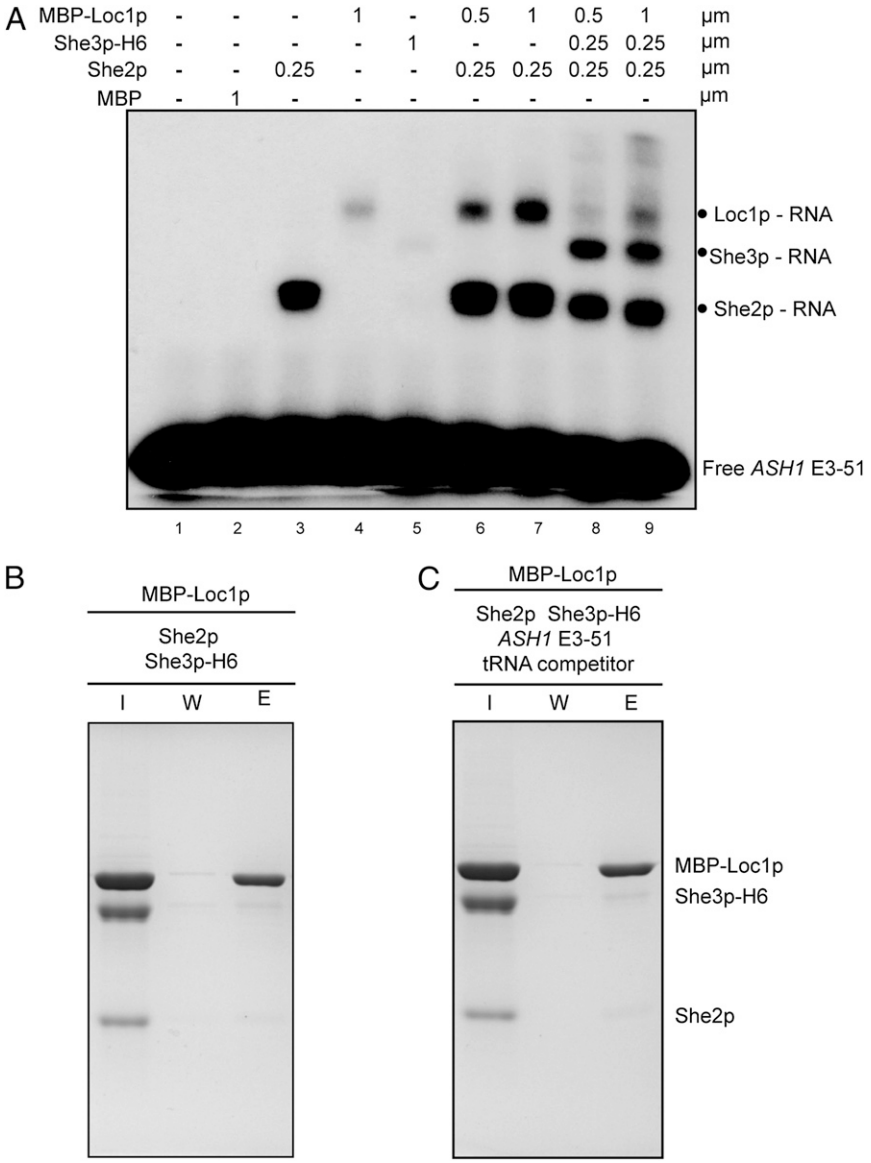

Fig. 5. She3p outcompetes Loc1p from the mRNP. (*A*) UV cross-linking experiment with She2p, She3p-H6, and MBP-Loc1p shows that in the presence of She2p and She3p Loc1p–RNA cross-linking is almost abolished. This finding suggests that She3p is able to outcompete Loc1p from its cocomplex with She2p and RNA, resulting in the synergistic cocomplex of She2p, She3p, and RNA (8), as well as free Loc1p. (*B*) Pull-down experiment with amylose resin and MBP-Loc1p, She2p, and She3p. None of the components can be pulled down efficiently with MBP-Loc1p, indicating that in the presence of She3p the protein interaction between Loc1p and She2p is disrupted. (*C*) Pull-down experiment with MBP-Loc1p, She2p, She3p-H6, *ASH1* E3-51 RNA, and tRNA competitor. Also in the presence of RNA, Loc1p is not able to form a cocomplex with any of these components.

Mutational Studies with She2p Indicate Overlapping Binding Sites of She3p and Loc1p. Because we observed an outcompetition of Loc1p by She3p, these proteins most likely share overlapping binding sites on She2p. To test this assumption we performed pull-down experiments with mutant versions of She2p. It was previously shown that the She2p mutation of leucine 130 into tyrosine [She2p (L130Y)] impairs its oligomeric state and its in vivo interaction with She3p (30). A recent study further showed that the deletion of the very C terminus of She2p [She2p (ΔC)] has no strong effect on in vitro binding to She3p, whereas the deletion of its protruding helix [She2p (ΔhE)] abolishes the She3p interaction (8). We first recapitulated these results (Fig. S6*A*) and then tested these mutant versions of She2p for Loc1p binding. We found that Loc1p shows reduced binding to She2p (L130Y), whereas She2p (ΔC) is bound like wild-type She2p (Fig. S6*B*). The observation that mutations in She2p affect Loc1p and She3p binding is consistent with the assumption that both proteins share an overlapping interaction surface on She2p.

Deletion of Cytoplasmic She3p Alters Nuclear Distribution of Loc1p. The observed displacement of Loc1p from the complex with She2p and *ASH1* E3 RNA by She3p (Fig. 5) suggests that this mechanism might also contribute in vivo to the removal of Loc1p from the *ASH1* mRNP. She3p has been previously shown to be exclusively cytoplasmic (8). First, we wanted to elucidate whether Loc1p is found at or close to the nuclear periphery, where an interaction with She3p could potentially occur. We performed double staining of GFP-tagged Loc1p and mCherry-tagged nuclear pore marker Nup120. As previously shown by Du et al. (14), Loc1p is clearly found in the nucleolus (Fig. 6*A*). The overlay with Nup120-mCherry shows that this nucleolar localization of Loc1p also reaches parts of the nuclear periphery.

If She3p is indeed necessary for removing Loc1p from *ASH1* mRNA during nuclear export, the Loc1p distribution should be altered in a *she3*Δ strain. Because the majority of Loc1p is likely involved in ribosome biogenesis inside the nucleolus, alterations in Loc1p distribution are expected to be relatively mild. We therefore overexpressed *ASH1* mRNA from a 2μ plasmid and

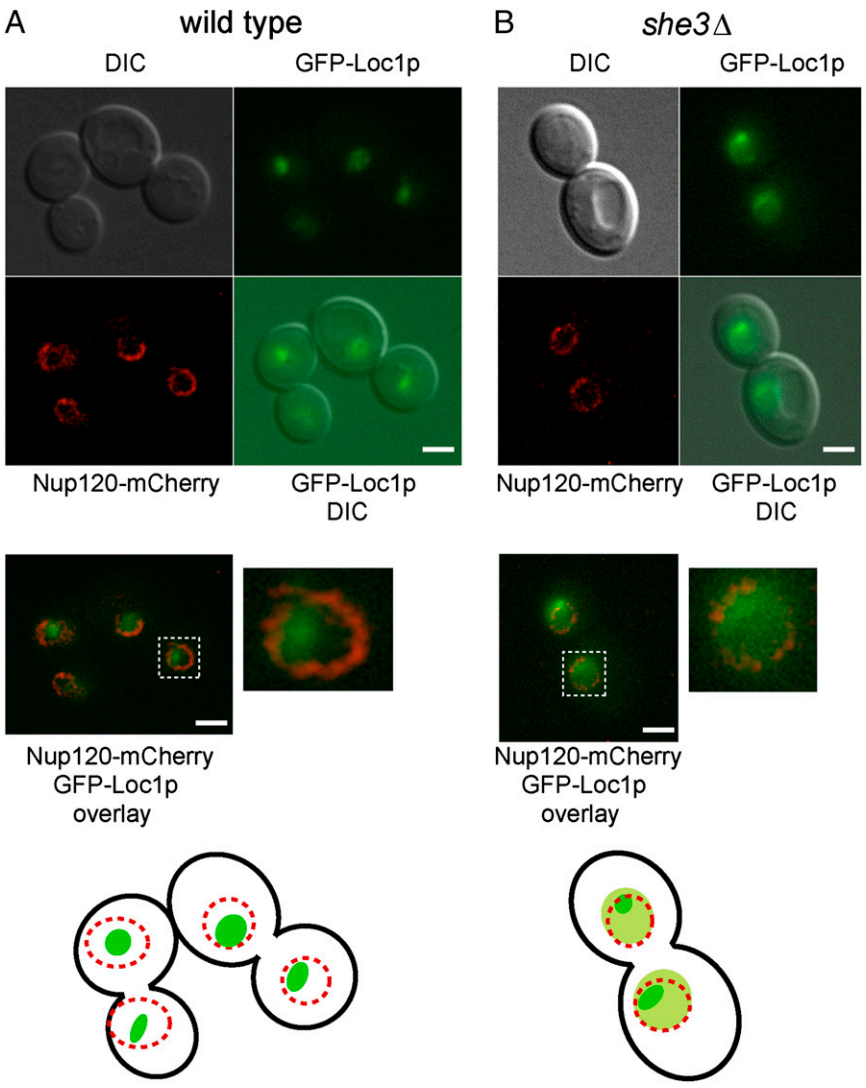

Fig. 6. (*A* and *B*) Localization of Loc1p in dividing wild-type (*A*) and *she3*Δ cells (*B*). Loc1p is visualized via GFP tag (green) and the nuclear envelope by Nup120-mCherry (red). (*A* and *B*, *Middle*) Overlays of Nup120-mCherry and GFP-Loc1p with magnifications of single cells. (Scale bars, 1 μm.) In wild-type cells (*A*), GFP-Loc1p shows a distinct localization in the nucleolus, as previously described (14, 15). In the *she3*Δ strain (*B*), part of the nucleolar Loc1p becomes dispersed in the nucleoplasm, demonstrating that cytoplasmic She3p influences the nuclear distribution of Loc1p. Occasionally, we also observed GFP-Loc1p signal in the cytoplasm of *she3*Δ cells. (*Bottom*) Cartoons illustrate the differences in Loc1p distribution.

focused on cells in anaphase when *ASH1* expression peaks (32). In these cells with wild-type She3p expression, GFP-Loc1p distribution is clearly limited to the nuclear crescent that is typical for the yeast nucleolus (Fig. 6*A*) (14). In contrast, cells that are deficient for She3p show a dispersed GFP-Loc1p staining in the nucleoplasm (Fig. 6*B*). This observation indicates that cytoplasmic She3p indeed affects Loc1p distribution in the nucle(ol)us. Occasionally, we also observed a weak cytoplasmic staining of GFP-Loc1p in *she3*Δ cells. However, this is an infrequent event and weaker than the nucleoplasmic staining in mutant cells.

Discussion

To date little is known about the molecular mechanisms involved in the early nuclear stages of localizing mRNPs and how nucleolar transitions are organized. Nucleolar trespassing of pre-mRNPs before cytoplasmic mRNA localization is not limited to the SHE complex in yeast. For instance, mammalian Staufen2 also passes through the nucleolus before its nuclear export (33). Here we present a study in which we systematically assessed the interplay between transport factors that associate with *ASH1* mRNA already in the nucleus. This allows us to provide a mechanistic understanding of these early events.

It was recently shown that the interaction of Loc1p and Puf6p with *ASH1* mRNA is impaired when She2p is prevented from entering the nucleus (19). This suggests interdependence between these protein–RNA interactions. Furthermore, Loc1p remains in the nucleus but is nevertheless important for cytoplasmic mRNA localization. Together, these findings indicate that the nuclear assembly of the pre-mRNP is important for cytoplasmic mRNA localization and translational repression.

A puzzling observation of previous studies was that the in vitro interaction between She2p and *ASH1* mRNA is very transient (8, 30). However, because She2p is cotranscriptionally recruited to *ASH1* mRNA (7, 8) and exported in an RNA-dependent manner to the cytoplasm (22), the formation of a stable complex in the nucleus is expected to occur. In the cytoplasm the interaction of *ASH1* mRNA and She2p is stabilized by the formation of a highly specific cocomplex with cytoplasmic She3p (8). An unresolved question is therefore whether and how She2p binding is modulated to form a stable complex with *ASH1* mRNA in the nucleus and whether such a nuclear complex would be specific for *ASH1* mRNA.

We found that She2p specifically binds to Loc1p even in the absence of RNA. We further observed a Loc1p-dependent stabilization of She2p binding to RNA. Loc1p alone shows only a modest preference for *ASH1* E3 RNA over HIV TAR-57 RNA (about 3-fold stronger K_d; Fig. 3*E*). However, Loc1p in cocomplex with She2p shows an about 40-fold better K_d for *ASH1* E3 RNA over HIV TAR-57 RNA, clearly indicating a specific selection of zip-code RNA.

Our pull-down experiments further indicated that zip-code–containing RNA is bound in a different mode by She2p and Loc1p than a control RNA (Fig. 3 *A* and *B* and Fig. S2*B*). In fact, ternary complexes formed only with zip-code RNA. Together with UV cross-linking and filter-binding assays, these findings suggest that Loc1p is required to stably and specifically associate She2p with nuclear *ASH1* mRNA. The cooperative, mutual recruitment and stabilization of Loc1p and She2p on the RNA are in agreement with the previous observation that in a nuclear localization-deficient She2p strain almost no *ASH1* mRNA was immunoprecipitated with TAP-tagged Loc1p (19).

An interesting question arising from these insights is where this stable ternary complex forms in the nucleus. For She2p a cotranscriptional recruitment to the *ASH1* mRNA has already been described (Fig. 7, *Upper*, A), whereas the exact location of Loc1p joining the early mRNP is unknown. One possible scenario is that Loc1p encounters She2p at or in the nucleolus, where Loc1p is enriched. Loc1p has a theoretical isoelectric point of 10.3, which is very similar to that of the vast majority of ribosomal proteins. Although nucleolar localization signals are difficult to predict (34), the considerable number of putative signals in Loc1p (Fig. S5) indicates that this protein is very likely localizing directly to the nucleolus without the need of a nucleolar hub protein. In contrast, She2p does not possess detectable nucleolar localization signals. Therefore, the interaction of Loc1p might not only stabilize She2p on the *ASH1* mRNA, but also piggyback She2p into the nucleolus (Fig. 7, *Upper*, A and B). Such indirect nucleolar recruitment mechanisms have been reported already for other proteins without intrinsic nucleolar localization signal, such as Nucleolin and Nucleophosmin (35).

Because She2p associates with *ASH1* mRNA already cotranscriptionally, it is also tempting to speculate that Loc1p binds to She2p already after or even before its association with the *ASH1* transcription complex in the nucleoplasm (Fig. 7, *Upper*, A). The recruitment of Loc1p could help to stably tether She2p to the *ASH1* mRNA already at the onset of mRNP biogenesis. This complex would remain associated until joining of She3p and formation of the She2p-She3p complex in the cytoplasm displaces Loc1p from the mRNP (see below).

In a mutant yeast strain with cytoplasmically trapped She2p, the nuclear interaction between Puf6p and *ASH1* mRNA is strongly impaired (19). In our in vitro assays we failed to observe a direct interaction of Puf6p with She2p or Loc1p or a recruitment of Puf6p by these factors to the *ASH1* mRNA. Hence, there must be another explanation for this dependence of Puf6p on She2p. Like for *puf6*Δ, the *LOC1* deletion strain exhibits defects in *ASH1* translational repression (13, 14). Furthermore, Puf6p shows a strong nucleolar enrichment (15) similar to that of Loc1p. Therefore, Loc1p-dependent piggybacking of She2p and *ASH1* mRNA into the nucleolus would be an obvious mechanism to bring the mRNP in the vicinity of Puf6p and to allow its loading into the complex (Fig. 7, *Upper*, C). Such a scenario would be consistent not only with our in vitro observations but also with the dependence of Puf6p binding to *ASH1* mRNA on She2p in vivo (19). Interestingly, Loc1p- as well as Puf6p-dependent translational repression is mediated by the E3 zip-code element (11, 21), indicating that this element fulfills a special function in *ASH1* mRNA.

After nucleolar trespassing, the *ASH1* mRNP is exported into the cytoplasm and Loc1p has to be removed from the *ASH1* mRNP. We observed that the cocomplex of She2p and She3p is able to displace Loc1p from the *ASH1* mRNP. She3p is strictly cytoplasmic and constitutively tethered to the cytoskeleton (8). Furthermore, with a molecular weight of 47 kDa She3p is too large to freely diffuse through the nuclear pore (36). Also the nuclear protein Loc1p was reported not to shuttle between nucleus and cytoplasm, as judged by shuttling and heterokaryon assays (13). Because these techniques are not very sensitive, minor subfractions might have remained undetected. Based on the observation that the deletion of *SHE3* does affect the nuclear localization and occasionally leads to cytoplasmic accumulation of Loc1p, it is conceivable that an outcompetition of Loc1p by the She2p-She3p cocomplex indeed occurs at or close to the nuclear pore (Fig. 7, *Upper*, D).

From the data presented here, we conclude that a stable and specific ternary complex is formed within the nucleus consisting of She2p, Loc1p, and *ASH1* mRNA. This pre-mRNP trespasses the nucleolus in a Loc1p-dependent manner. Because we do not observe a direct interaction of Puf6p with the pre-mRNP constituents or recruitment to the *ASH1* mRNA, it seems likely that Puf6p joins the mRNP independently, probably within the nucleolus. After nucleolar trespassing, the mRNP is exported into the cytoplasm, where the mature transport complex together with She3p and Myo4p is formed. Our data implicate that She3p outcompetes Loc1p for the interaction with She2p and *ASH1* mRNA during or shortly after nuclear export. The reported assembly line of the nuclear mRNP ensures that all required factors associate and dissociate at the right time to

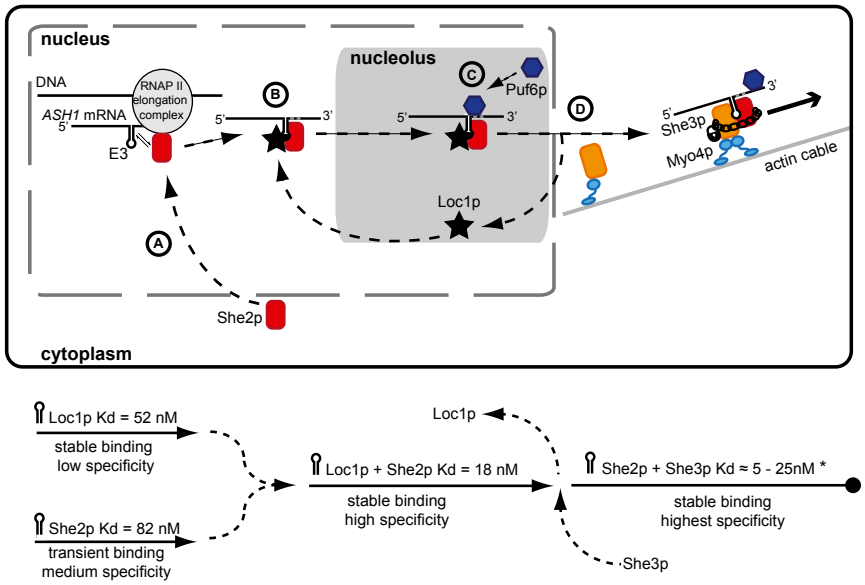

Fig. 7. Model for sequential binding and release of Loc1p to the *ASH1* mRNP. (*Upper*) She2p enters the nucleus and binds cotranscriptionally to the *ASH1* mRNA (A). Loc1p joins this subcomplex, which leads to stabilization of She2p on the *ASH1* mRNA. Loc1p contains nucleolar localization signals and is strongly enriched in the nucleolus, suggesting that it recruits She2p into the nucleolus through their direct interaction (B). No direct interaction between Puf6p and other core factors could be detected in this study. Nevertheless, in vivo the *ASH1* mRNA association of Puf6p depends on She2p. It is likely that Loc1p and She2p are required to recruit *ASH1* mRNA into the nucleolus, where Puf6p can interact with the transcript (C). Because Loc1p is not part of the cytoplasmic transport complex, it has to be removed from the complex before or during nuclear export (D). The synergistic cocomplex of She2p and She3p outcompetes Loc1p from the mRNP and ensures that Loc1p is absent from the cytoplasmic *ASH1* transport complex. (*Lower*) Schematic drawing of the changes of RNA-binding properties during the stepwise assembly of the *ASH1* mRNP. In particular, the affinity and specificity, but also complex stability, improve from the initial nuclear binding events to the assembly of the mature cytoplasmic transport complex. This gradient in binding properties is suitable to explain the directionality of complex maturation. Asterisk indicates that this K_d has been estimated from figure 3C of ref. 8.

escort the *ASH1* mRNA from its site of transcription all of the way to its localization at the bud tip.

Materials and Methods

Protein Expression and Purification. Full-length Loc1p was expressed with an N-terminal MBP-tag or H6-tag in *Escherichia coli* strain BL21 (DE3). After induction with 0.25 mM isopropyl β-D-1-thiogalactopyranoside in the logarithmic growth phase cells were cultured for 16 h at 18 °C and harvested. Cells were sonicated at 4 °C in lysis buffer (20 mM Hepes, pH 7.4, 500 mM KCl, 0.5 mM EDTA, complete protease inhibitor or 20 mM K-Phosphate, pH 7.5, 500 mM KCl, 50 mM Imidazole, and complete protease inhibitor). After centrifugation the clarified supernatant was applied to an amylose/Ni Sepharose resin column and washed with high-salt buffer (1 M KCl) to remove nucleic acids and subsequently with low-salt buffer (150 mM KCl). The protein was eluted with 20 mM maltose or 750 mM imidazole in low-salt buffer and further purified using ion exchange chromatography (SP FF; GE Healthcare), heparin affinity chromatography, and size exclusion chromatography (e.g., Superdex S200; GE Healthcare).

Full-length She2p and Puf6p were expressed and purified as GST-fusion proteins in *E. coli* strain BL21 (DE3) and purified as previously described (8, 37).

His_6-tagged She3p was coexpressed with She2p in insect cells (High Five) using the bac-to-bac system (Invitrogen) and purified with affinity, ion exchange, and size exclusion chromatography as previously described (8). Plasmids and primers used in this study are listed in Tables S1 and S2.

To remove RNA contaminations from each of the above-mentioned proteins, a high-salt washing step was carried out during the affinity chromatography and validated via measurement of the OD_{254} to OD_{280} ratio. Proteins with an OD_{254} to OD_{280} ratio below 0.6 were specified as RNA/DNA free.

RNA Preparation. RNA was produced by in vitro transcription (E3-118), tRNA scaffold expression, and purification (E3-51 tRNA, E3-118 tRNA, and TAR-57 tRNA) or total chemical synthesis (E3-51; Dharmacon) (38). For in vitro transcription the 118-nt DNA fragment of the *ASH1* gene (plasmid pRS405-*ASH1* in Table S1) was PCR amplified using primers with the T7 promotor sequence at the 5′ end. This fragment was used as a template for in vitro transcription (MEGAshortscript Kit; Ambion). The transcribed RNA was purified as described in the manufacturer's instructions, using DNase digestion, phenolic extraction, and ethanol precipitation. The integrity of the RNA was confirmed by agarose gel electrophoresis.

$tRNA_{Met}$ fusion constructs (E3-51 tRNA, E3-118 tRNA, and TAR-57 tRNA) were overexpressed in *E. coli* JM 101 cells, using 2x typtone-yeast media. The RNA was phenol-chloroform extracted, ethanol precipitated, and further purified by ion exchange chromatography (DAEA and MonoQ columns), as described in ref. 29. Pure fractions were identified by 8% (vol/vol) Tris/borate/EDTA (TBE) Urea PAGE, pooled, and ethanol precipitated.

For UV cross-linking and EMSA experiments in vitro-transcribed E3-118 zip-code RNA, synthesized E3-51, or recombinant E3-51 tRNA, E3-118 tRNA, or HIV TAR-57 tRNA constructs were radioactively labeled using [γ^{32}P]ATP and T4 polynucleotide kinase. Free nucleotides were separated from the RNA, using either Sepharose spin columns (NucAway; Ambion, E3-51 element) or phenol-chloroform extraction (E3-118, E3-51 tRNA, E3-118 tRNA, and HIV TAR-57 tRNA). For interaction studies with Puf6p the E3-118 or E3-118 tRNA zip-code RNA was used, because it includes the corresponding Puf6p binding element (11). For interaction studies without Puf6p the E3-51 zip-code element was used because of better recovery rates after isotope labeling. The sequences of RNAs used in this study are listed in Table S3.

EMSA. In a total volume of 20 μL 5 nM radioactively labeled RNA, 100 μg/mL tRNA competitor, and the indicated protein concentration were mixed in HNMD buffer (20 mM Hepes, pH 7.8, 200 mM NaCl, 2 mM $MgCl_2$, 2 mM DTT) with 4% glycerol. After 25 min incubation at 25 °C the RNA protein complexes were resolved by native TBE PAGE (6% polyacrylamide, 1× TBE running buffer). Gels were incubated for 15 min in fixing solution [10% (vol/vol) acetic acid, 30% (vol/vol) methanol] and vacuum dried. Gels were analyzed with radiograph films. For supershift EMSAs monoclonal She2p antibody (30) was included in the reaction. DTT was omitted from the HNMD reaction buffer for supershift EMSAs. For detection of cocomplexes 4–20% TBE gradient gels were used.

UV Cross-Linking Experiments. In a total volume of 20 μL 5 nM radiolabeled RNA, 100 μg/mL tRNA, and the indicated protein concentrations were mixed in HNMD buffer. After 25 min incubation at 25 °C the samples were subjected to 2.25 J UV radiation over 15 min on ice. The distance between the samples and the UV lamp was ~8 cm. After adding SDS loading dye, samples were incubated for 5 min at 90 °C and separated on 10% SDS/PAGE. Gels were fixed, dried, and analyzed with radiograph films.

In Vitro Pull-Down Experiments. In a total volume of 100 μL 7.5 or 10 μM protein, 4 μM E3-51/E3-118 tRNA, and 5 mg/mL yeast tRNA competitor (unless stated otherwise) as indicated were mixed in appropriate pull-down buffer (20 mM Hepes, pH 7.8, 150 mM or 200 mM NaCl, 2 mM $MgCl_2$, 2 mM DTT or 20 mM K phosphate, pH 7.5, 150 mM or 200 mM KCl, 2 mM $MgCl_2$, and 30 mM imidazole). Samples were centrifuged for 10 min and supernatant was incubated for 30 min at 4 °C on a rotating wheel with 50 μL amylose resin (MBP-Loc1p), GST-Sepharose (GST-Puf6p), or Ni-NTA (She3p-H6). Binding reactions were washed four times with 200 μL and once with 50 μL pull-down buffer. Bound proteins were eluted with maltose (amylose resin), glutathione (GST-Sepharose), or imidazole (Ni-NTA). On SDS/PAGE 10% of the input, 20% of the last wash step, and 20% of the elution were analyzed by Coomassie blue staining. RNA was analyzed on a 1.5% agarose gel or an urea PAGE with GelRed DNA stain, according to ref. 38.

Filter-Binding Assays. In a total volume of 80 μL the indicated protein concentrations and 0.5 nM of radiolabeled RNA (*ASH1* E3-51 tRNA, HIV TAR-57 tRNA) were incubated for 25 min in filter-binding buffer (10 mM Hepes, pH 7.4, 100 mM NaCl, 1 mM DTT, and 5 mM $MgCl_2$) supplemented with 30 μg/mL yeast tRNA competitor. Samples were applied to nitrocellulose and nylon membranes, using a Dot Blot Aparatus (BioRad), and washed twice with filter-binding buffer. Membranes were air dried and analyzed by phosphoimaging. Quantification of signal intensities was carried out using the Dot Blot Analyzer macro within the ImageJ program and further analyzed with the program Origin 8.6.

Generation of Yeast Strains. Strain RJY4358 (LOC1-GFP::HIS3MX6) was generated by one-step tagging of W303a according to ref. 39. To construct strain RJY4359 (LOC1-GFP::HIS3MX6 *she3*Δ::URA3), RJY4358 was transformed with a DNA construct containing the URA3 gene flanked by sequences of the 5′ and 3′ regions of SHE3, which was obtained by PCR amplification from the *she3*Δ::URA3 locus of strain RJY90 (40). Before imaging, both strains were transformed with plasmid pRJ88 (YEplac181-ASH1), which allows overexpression of *ASH1* mRNA during mitosis, and plasmid pRS314-Nup120-mCherry, which allows detection of nuclear pores. Genotypes of used yeast strains as well as plasmids for transformation are listed in Tables S1 and S4.

In Vivo Imaging. For imaging, a single yeast colony from a fresh plate grown at 30 °C was inoculated in 1 mL of synthetic complete (SC) medium with 2% glucose but lacking leucine and tryptophane. Cells were grown at 30 °C for 4–4.5 h to enrich for mitotic cells. Cells were collected by short spin and resuspended in 100 μL of SC medium. One microliter of cell suspension was placed on a multiwell slide coated with agarose before microscopic observation. For each mitotic cell pair, Z-stacks containing 50 images at 200-nm distance were acquired for GFP, mCherry, and DIC. Due to the weaker signal of Nup120-mCherry, mCherry images were deconvoluted before mounting. Image processing and mounting were performed with AxioVision software version 4.8 (Zeiss). GFP and mCherry overlay pictures were generated using Adobe Photoshop CS3. Essentially the mCherry Layer was duplicated and inserted in the GFP file. By using exclusion in the layer option an overlay was generated and one representative cell was magnified.

ACKNOWLEDGMENTS. We thank Sigrun Jaklin and Vera Roman for their support. We thank Ed C. Hurt for generously providing the plasmid pRS 314-Nup120-mCherry. This work was supported by the Deutsche Forschungsgemeinschaft (A.N., R.-P.J., and D.N.), the Helmholtz Association (Grant NG-VH142 to D.N.), the Bayerisch-Französisches Hochschulzentrum (A.N. and D.N.), and the Boehringer-Ingelheim Fonds (M.M.).

1. Holt CE, Bullock SL (2009) Subcellular mRNA localization in animal cells and why it matters. *Science* 326(5957):1212–1216.
2. St Johnston D (2005) Moving messages: The intracellular localization of mRNAs. *Nat Rev Mol Cell Biol* 6(5):363–375.
3. Jansen RP, Niessing D (2012) Assembly of mRNA-protein complexes for directional mRNA transport in eukaryotes—an overview. *Curr Protein Pept Sci* 13(4):284–293.
4. Niessing D, et al. (1997) A cascade of transcriptional control leading to axis determination in Drosophila. *J Cell Physiol* 173(2):162–167.
5. Heym RG, Niessing D (2012) Principles of mRNA transport in yeast. *Cell Mol Life Sci* 69(11):1843–1853.
6. Paquin N, Chartrand P (2008) Local regulation of mRNA translation: New insights from the bud. *Trends Cell Biol* 18(3):105–111.
7. Shen Z, St-Denis A, Chartrand P (2010) Cotranscriptional recruitment of She2p by RNA pol II elongation factor Spt4-Spt5/DSIF promotes mRNA localization to the yeast bud. *Genes Dev* 24(17):1914–1926.
8. Müller M, et al. (2011) A cytoplasmic complex mediates specific mRNA recognition and localization in yeast. *PLoS Biol* 9(4):e1000611.
9. Deng Y, Singer RH, Gu W (2008) Translation of ASH1 mRNA is repressed by Puf6p-Fun12p/eIF5B interaction and released by CK2 phosphorylation. *Genes Dev* 22(8):1037–1050.
10. Paquin N, et al. (2007) Local activation of yeast ASH1 mRNA translation through phosphorylation of Khd1p by the casein kinase Yck1p. *Mol Cell* 26(6):795–809.
11. Gu W, Deng Y, Zenklusen D, Singer RH (2004) A new yeast PUF family protein, Puf6p, represses *ASH1* mRNA translation and is required for its localization. *Genes Dev* 18(12):1452–1465.
12. Irie K, et al. (2002) The Khd1 protein, which has three KH RNA-binding motifs, is required for proper localization of *ASH1* mRNA in yeast. *EMBO J* 21(5):1158–1167.
13. Long RM, et al. (2001) An exclusively nuclear RNA-binding protein affects asymmetric localization of *ASH1* mRNA and Ash1p in yeast. *J Cell Biol* 153(2):307–318.
14. Du TG, et al. (2008) Nuclear transit of the RNA-binding protein She2 is required for translational control of localized ASH1 mRNA. *EMBO Rep* 9(8):781–787.
15. Huh WK, et al. (2003) Global analysis of protein localization in budding yeast. *Nature* 425(6959):686–691.
16. Urbinati CR, Gonsalvez GB, Aris JP, Long RM (2006) Loc1p is required for efficient assembly and nuclear export of the 60S ribosomal subunit. *Mol Genet Genomics* 276(4):369–377.
17. Ho Y, et al. (2002) Systematic identification of protein complexes in Saccharomyces cerevisiae by mass spectrometry. *Nature* 415(6868):180–183.
18. De Marchis ML, Giorgi A, Schininà ME, Bozzoni I, Fatica A (2005) Rrp15p, a novel component of pre-ribosomal particles required for 60S ribosome subunit maturation. *RNA* 11(4):495–502.
19. Shen Z, Paquin N, Forget A, Chartrand P (2009) Nuclear shuttling of She2p couples ASH1 mRNA localization to its translational repression by recruiting Loc1p and Puf6p. *Mol Biol Cell* 20(8):2265–2275.
20. Oeffinger M, et al. (2007) Comprehensive analysis of diverse ribonucleoprotein complexes. *Nat Methods* 4(11):951–956.
21. Komili S, Farny NG, Roth FP, Silver PA (2007) Functional specificity among ribosomal proteins regulates gene expression. *Cell* 131(3):557–571.
22. Kruse C, et al. (2002) Ribonucleoprotein-dependent localization of the yeast class V myosin Myo4p. *J Cell Biol* 159(6):971–982.
23. Böhl F, Kruse C, Frank A, Ferring D, Jansen RP (2000) She2p, a novel RNA-binding protein tethers *ASH1* mRNA to the Myo4p myosin motor via She3p. *EMBO J* 19(20):5514–5524.
24. Heuck A, et al. (2007) Monomeric myosin V uses two binding regions for the assembly of stable translocation complexes. *Proc Natl Acad Sci USA* 104(50):19778–19783.
25. Heuck A, et al. (2010) The structure of the Myo4p globular tail and its function in ASH1 mRNA localization. *J Cell Biol* 189(3):497–510.
26. Hodges AR, Krementsova EB, Trybus KM (2008) She3p binds to the rod of yeast myosin V and prevents it from dimerizing, forming a single-headed motor complex. *J Biol Chem* 283(11):6906–6914.
27. Long RM, Gu W, Lorimer E, Singer RH, Chartrand P (2000) She2p is a novel RNA-binding protein that recruits the Myo4p-She3p complex to *ASH1* mRNA. *EMBO J* 19(23):6592–6601.
28. Takizawa PA, Vale RD (2000) The myosin motor, Myo4p, binds *Ash1* mRNA via the adapter protein, She3p. *Proc Natl Acad Sci USA* 97(10):5273–5278.
29. Ponchon L, Beauvais G, Nonin-Lecomte S, Dardel F (2009) A generic protocol for the expression and purification of recombinant RNA in Escherichia coli using a tRNA scaffold. *Nat Protoc* 4(6):947–959.
30. Müller M, et al. (2009) Formation of She2p tetramers is required for mRNA binding, mRNP assembly, and localization. *RNA* 15(11):2002–2012.
31. Wong I, Lohman TM (1993) A double-filter method for nitrocellulose-filter binding: Application to protein-nucleic acid interactions. *Proc Natl Acad Sci USA* 90(12):5428–5432.
32. Bobola N, Jansen RP, Shin TH, Nasmyth K (1996) Asymmetric accumulation of Ash1p in postanaphase nuclei depends on a myosin and restricts yeast mating-type switching to mother cells. *Cell* 84(5):699–709.
33. Macchi P, et al. (2004) The brain-specific double-stranded RNA-binding protein Staufen2: Nucleolar accumulation and isoform-specific exportin-5-dependent export. *J Biol Chem* 279(30):31440–31444.
34. Sirri V, Urcuqui-Inchima S, Roussel P, Hernandez-Verdun D (2008) Nucleolus: The fascinating nuclear body. *Histochem Cell Biol* 129(1):13–31.
35. Emmott E, Hiscox JA (2009) Nucleolar targeting: The hub of the matter. *EMBO Rep* 10(3):231–238.
36. Görlich D, Kutay U (1999) Transport between the cell nucleus and the cytoplasm. *Annu Rev Cell Dev Biol* 15:607–660.
37. Niessing D, Hüttelmaier S, Zenklusen D, Singer RH, Burley SK (2004) She2p is a novel RNA binding protein with a basic helical hairpin motif. *Cell* 119(4):491–502.
38. Edelmann FT, Niedner A, Niessing D (2013) Production of pure and functional RNA for in vitro reconstitution experiments. *Methods*, 10.1016/j.ymeth.2013.08.034.
39. Janke C, et al. (2004) A versatile toolbox for PCR-based tagging of yeast genes: New fluorescent proteins, more markers and promoter substitution cassettes. *Yeast* 21(11):947–962.
40. Jansen RP, Dowzer C, Michaelis C, Galova M, Nasmyth K (1996) Mother cell-specific HO expression in budding yeast depends on the unconventional myosin myo4p and other cytoplasmic proteins. *Cell* 84(5):687–697.

Supporting Information

Niedner et al. 10.1073/pnas.1315289111

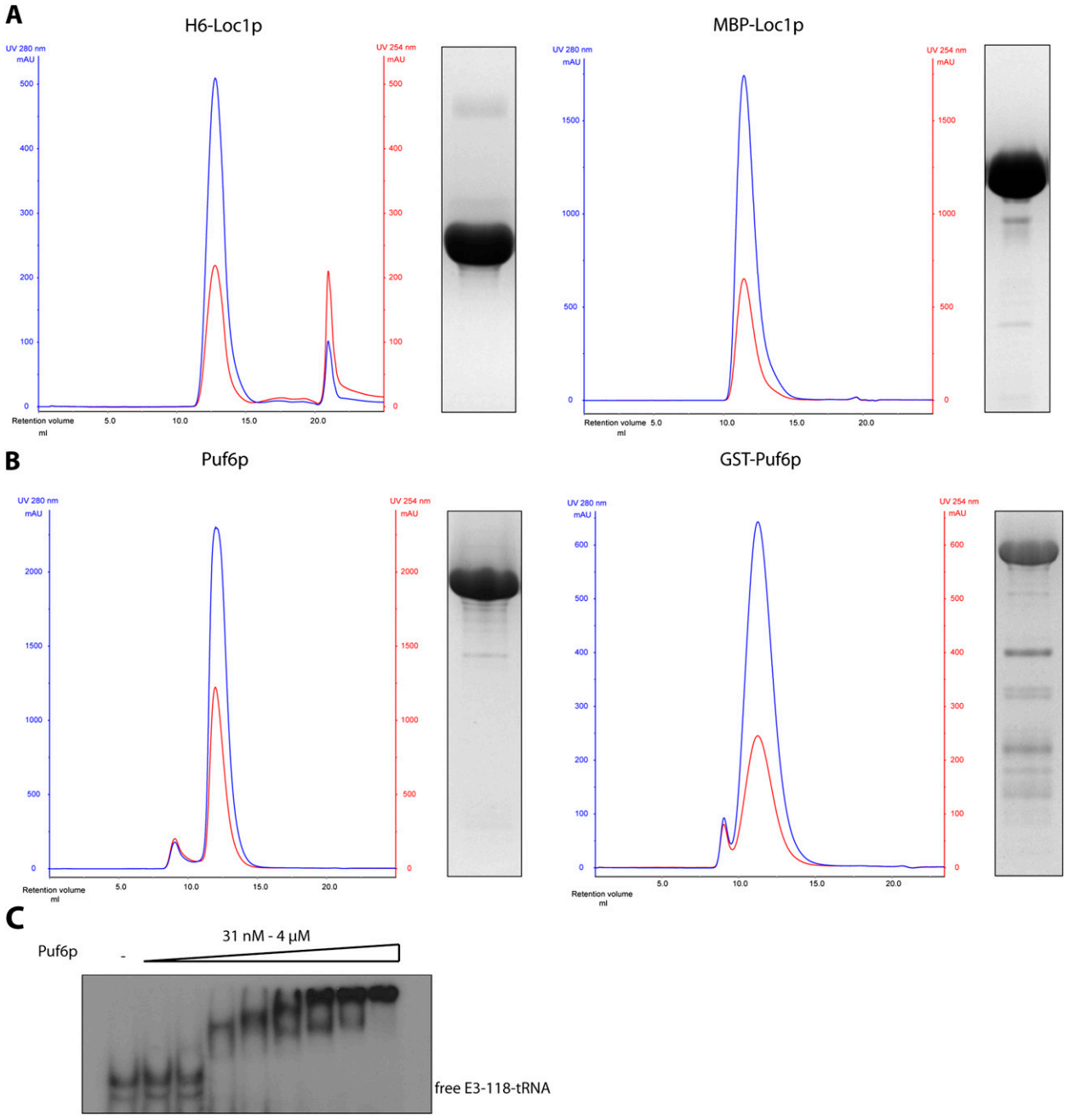

Fig. S1. Recombinantly expressed and purified proteins show high purity and are functional. (*A*) Size-exclusion chromatograms and corresponding SDS/PAGE gels stained with Coomassie blue show that His-tagged localization of asymmetric synthesis of HO 1 (*ASH1*) mRNA protein 1 (H6-Loc1p) and maltose binding protein (MBP)-Loc1p are highly pure. Observe the absorbance ratios at 254 nm (red) and 280 nm (blue) in the chromatograms, indicating that purified proteins are free of nucleic acids. Only proteins with absorbance ratios of 254/280 $\leq$ 0.6 were used for experiments. (*B*) Size-exclusion chromatograms and corresponding SDS/PAGE stained with Coomassie blue show that untagged pumilio-homology domain family protein 6 (Puf6p) is highly pure and GST-Puf6p reasonable pure. Protein preparations were free of nucleic acids. (*C*) Electrophoretic mobility-shift assay (EMSA) showing that untagged Puf6p efficiently binds to radioactively labeled *ASH1* E3-118 tRNA. This observation is consistent with previous reports (1, 2) and proves the functional activity of purified Puf6p.

1. Gu W, Deng Y, Zenklusen D, Singer RH (2004) A new yeast PUF family protein, Puf6p, represses *ASH1* mRNA translation and is required for its localization. *Genes Dev* 18(12):1452–1465.
2. Müller M, et al. (2011) A cytoplasmic complex mediates specific mRNA recognition and localization in yeast. *PLoS Biol* 9(4):e1000611.

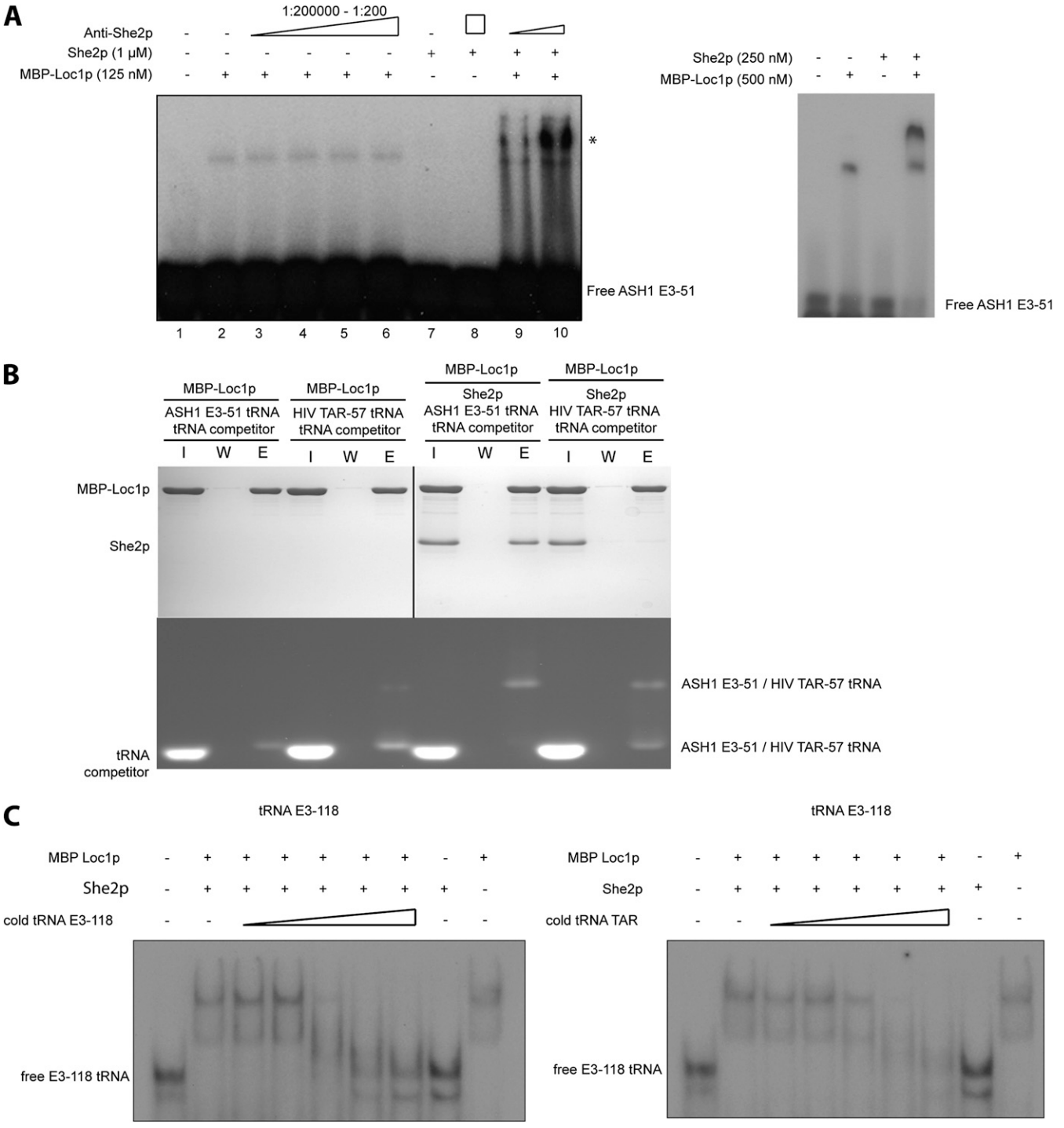

Fig. S2. EMSAs with Loc1p, Swi5p-dependent HO expression protein 2 (She2p), and *ASH1* E3 RNA. (*A*) (*Left*) Supershift EMSA with MBP-Loc1p, She2p, She2p antibody and radioactively labeled *ASH1* E3-51 RNA. Loc1p alone (lane 2) and with increasing concentrations of She2p antibody (lanes 3–6) shows one weak and constant band shift without any supershift. She2p alone at 1 μM concentration (lane 7) and in combination with She2p and 1:200 dilution of antibody (lane 8) does not yield a band shift. The combination of Loc1p, She2p, and antibody dilutions (1:200,000 and 1:20,000) leads to the formation of a supershift (lanes 9 and 10, marked with an asterisk). The supershift increases in intensity at elevated antibody concentration, indicating the presence of She2p in this complex. (*Right*) An EMSA using a 4–20% gradient gel, which resolves the different RNA–protein complexes well enough to show a higher molecular weight band for the ternary complex of MBP-Loc1p, She2p, and *ASH1* E3-51 RNA. (*B*) Pull-down experiments with MBP-Loc1p as bait and *ASH1* E3-51 tRNA, HIV TAR-57 tRNA, and She2p as prey. MBP-Loc1p alone binds *ASH1* E3-51 tRNA as well as HIV TAR-57 tRNA and thus shows no specificity in pull-down experiments. However, She2p is retained on amylose beads only in the presence of *ASH1* E3-51, indicating a preference of this ternary complex for zip-code RNA. Note that in the RNA gels stable ternary complexes are observed that migrate at a higher molecular weight, similar to the observations in Fig. 3*A* (asterisk). For further details, see legend of Fig. 3*A*. (*C*) EMSAs with excess of unlabeled cold competitor RNA show that the complex consisting of Loc1p and She2p has a preference for RNAs with zip-code elements. For competition experiments we used 1-, 2-, 5-, 25-, and 50-fold excess of cold competitor RNA over labeled E3 zip-code RNA. Because these competition experiments gave only a rough indication, more quantitative approaches were used to assess complex specificity (Fig. 3 *D–F*).

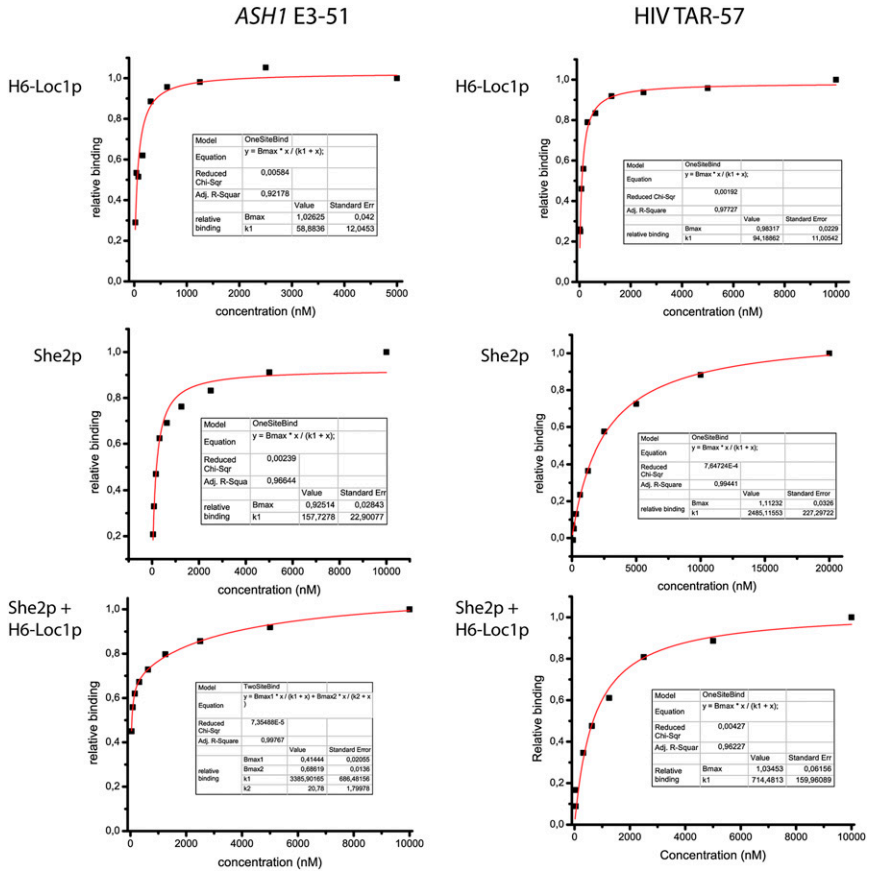

Fig. S3. Representative plots of binding curves from filter-binding assays for the determination of equilibrium-dissociation constants (K_d). Signal intensities of each black box are plotted over the respective protein concentration. K_ds were determined using either one-site binding or two-site binding fitting algorithms with the program Origin 8.6. Shown are representative fitting curves from individual experiments, with the respective fitting algorithms indicated in *Insets*. In binding experiments with individual proteins and RNA a one-site binding algorithm was used. However, the ternary complex formed by Loc1p, She2p, and E3 zip-code RNA requires a higher-order fitting function (two-site binding), indicating the presence of two RNA-interaction sites in this complex. This assumption is supported by cross-linking experiments showing that Loc1p as well as She2p contacts the *ASH1* E3 RNA upon complex formation (Fig. 2*A*). In contrast to the *ASH1* E3 zip-code RNA, data fitting of HIV-TAR binding to Loc1p and She2p demanded only a one-site binding algorithm, suggesting the absence of a ternary complex. This interpretation is consistent with those of pull-down assays (Fig. 3*B* and Fig. S2*B*) and cross-linking experiments (Fig. 3*C*).

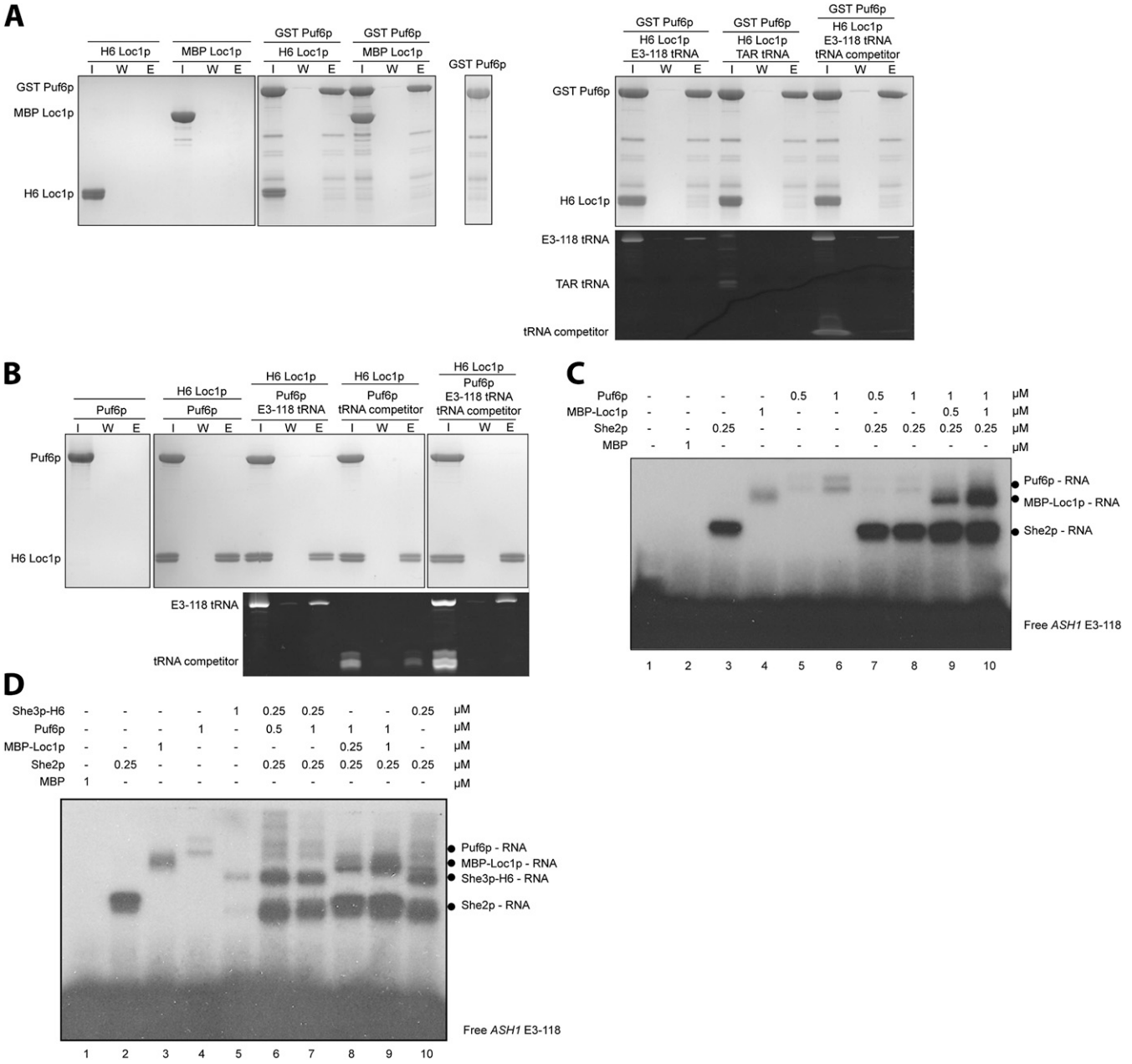

Fig. S4. Puf6p binds the *ASH1* E3 zip-code element but fails to interact with Loc1p in the absence or the presence of the *ASH1* E3 zip-code element. (*A*) Pull-down experiments with GST-Puf6p as bait and MBP-Loc1p or H6-Loc1p as prey in the presence or the absence of specific and unspecific RNA. No interaction between Loc1p and Puf6p is detected. In these experiments, more physiological pull-down conditions were applied than in Fig. 1. A total of 250 nM of each protein in 1.5 mL reaction volume was used with 50 µL of respective resin material. (*B*) Pull-down experiments with H6-Loc1p as bait and untagged Puf6p in the presence or the absence of *ASH1* E3 zip-code RNA as prey. No direct or RNA-mediated indirect interaction is observed between Loc1p and Puf6p either in the absence of RNA or in the presence of specific *ASH1* E3-118 tRNA or unspecific tRNAs. This further confirms the lack of a stable interaction between both molecules. These experiments were performed at the concentrations and volumes described in *A*. (*C*) Cross-linking experiment showing that Puf6p is not recruited to the *ASH1* E3 zip-code element by She2p alone (lanes 7 and 8) or by the She2p-Loc1p complex (lanes 9 and 10). Experimental conditions are identical to those in Figs. 2*A* and 4*C*. (*D*) Same cross-link as in Fig. 4*C* with prolonged exposure.

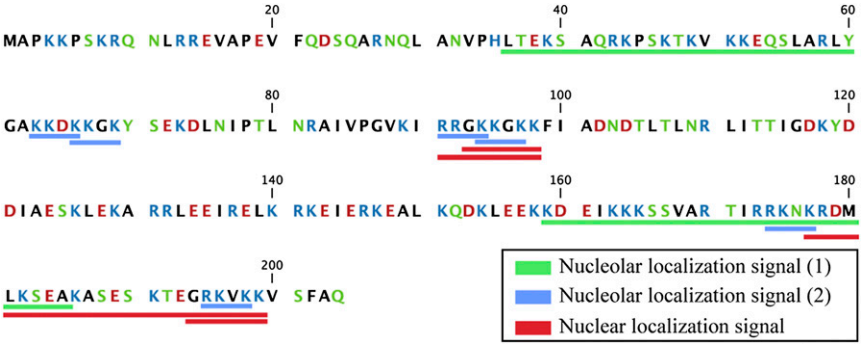

Fig. S5. Protein sequence of Loc1p and its predicted nucleolar and nuclear localization signals. Amino acids underlined in green have an extended nucleolar localization signal, as predicted by the program NoLS (1). Because NoLS has been designed to identify mammalian nucleolar localization signals, we also searched for more general nucleolar localization signals with the motif (K/R)(K/R)X(K/R) (blue) (2). Nuclear localization signals are depicted in red.

1. Scott MS, Boisvert FM, McDowall MD, Lamond AI, Barton GJ (2010) Characterization and prediction of protein nucleolar localization sequences. *Nucleic Acids Res* 38(21):7388–7399.
2. Horke S, Reumann K, Schulze C, Grosse F, Heise T (2004) The La motif and the RNA recognition motifs of human La autoantigen contribute individually to RNA recognition and subcellular localization. J Biol Chem 279(48):50302-50309.

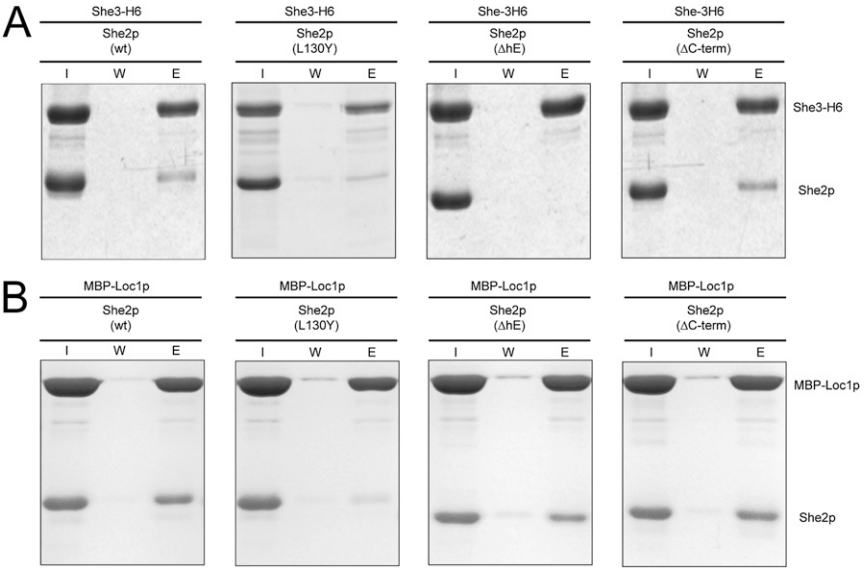

Fig. S6. Different She2p mutants that affect She3p binding also impair Loc1p binding. (*A*) In pull-down experiments with Ni-Sepharose resin and She3p-H6 the proteins She2p (WT) and She2p (ΔC-term) were efficiently copurified. In contrast, She3p does not interact with She2p (ΔhE) and has a weakened interaction with She2p (L130Y). (*B*) Amylose pull-down experiments with MBP-tagged Loc1p and She2p mutants. Whereas Loc1p showed reduced affinity for She2p (L130Y) and might have a slightly impaired interaction with She2p (ΔhE), wild-type–like binding was observed with She2p (ΔC-term). Together with competition experiments, these findings suggest that Loc1p and She3p use an overlapping but nonidentical binding surface on She2p.

Table S1. Plasmids

Plasmid name	Description	Source	PCR primers	Restriction sites
P01	pGEX-6p1 *SHE2*	(1)		
P06	pGEX-6p1 *she2* Δ C-term	(2)		
P08	pGEX-6p1 *she2* L130Y	(2)		
P14	pGEX-6p1 *she2* ΔhelixE	(2)		
P59	pET-28a *LOC1*	This study	MMO 103, MMO 104	BamHI, XhoI
P65	pET-M43 *LOC1*	This study	MMO 103, MMO 104	BamHi, XhoI
P94	pGEX-6p1 *PUF6*	(2)		
RHP 27	pFastBacDual-*SHE2*/*SHE3*-His6	(2)		
RHP 89	pBSMrna-E3-118	(2)		
RHP 90	pBSMrna-E3-51	This study	RHO 126, RHO 127	EagI, SacII
RHP 99	pBSMrna-HIV1-TAR	This study	RHO 134, RHO 135	EagI, SacII
ANP 11	pRS405-ASH1	This study	ANO 18, ANO 19	XhoI, BamHI
C3319	YEplac181-ASH1	(3)		
	pRS 314-Nup120-mCherry	(4)		

1. Niessing D, Hüttelmaier S, Zenklusen D, Singer RH, Burley SK (2004) She2p is a novel RNA binding protein with a basic helical hairpin motif. *Cell* 119(4):491–502.
2. Müller M, et al. (2011) A cytoplasmic complex mediates specific mRNA recognition and localization in yeast. *PLoS Biol* 9(4):e1000611.
3. Long RM, et al. (1997) Mating type switching in yeast controlled by asymmetric localization of *ASH1* mRNA. *Science* 277(5324):383–387.
4. Skruzný M, et al. (2009) An endoribonuclease functionally linked to perinuclear mRNP quality control associates with the nuclear pore complexes. *PLoS Biol* 7(1):e8.

Table S2. DNA oligonucleotides

Name	Primer sequence, 5′–3′
MMO 103	AAAAGGATCCATGGCACCAAAGAAACCTTC
MMO 104	AAAACTCGAGCTATTGAGCAAATGAGAC
RHO 126	AAACGGCCGATGGATAACTGAATCTCTTTCAAC
RHO 127	AAACCGCGGCCAATTGTTTCGTGATAATGTCTC
RHO 134	AAACGGCCGGGTCTCTCTGGTTAGACCAGATCTGAGCCTGGGAGCTCTCTGGCTAACTAGGGAACCTGGCCGCGGAAA
RHO 135	TTTCCGCGGCCAGGTTCCCTAGTTAGCCAGAGAGCTCCCAGGCTCAGATCTGGTCTAACCAGAGAGACCCGGCCGTTT
ANO 18	AAAAAACTCGAGTCCTGTCCTATCCTTATTACGTTCA
ANO 19	AAAAAAGGATCCTGCGCAGGAGAAGTTATTAGAATGAT

Table S3. RNA sequences

RNA	Base relative to start AUG	Sequence, 5′–3′	Produced by
ASH1 E3-118	1,750–1,867	GAGACAGUAGAGAAUUGAUAC AUGGAUAACUGAAUCUCUUUCA ACUAAUAAGAGACAUUAU CACGAAACAA**UUGU**ACAU UUCUCUCC**UUGU**CUGUGCUA AAUAAACUACAAAUAAAAA	In vitro transcription
ASH1 E3-118 tRNA	1,750–1,867	GGCUACGUAGCUCAGUU GGUUAGAGCAGCGGCCGGAG ACAGUAGAGAAUUGA UACAUGGAUAACUGAAUCUC UUUCAACUAAUAAGAGACAUUAUCA CGAAACAAUUGUACAUUUC UCUCCUUGUCUGUGCUAA AUAAACUACAAAUAAAAAUG GCCGCGGGUCACAGGUUCGA AUCCCGUCGUAGCCACCA	Expression in *Escherichia coli*
ASH1 E3-51 tRNA	1,771–1,821	GGCUACGUAGCUCAGUUG GUUAGAGCAGCGGCCG AUGGAUAACUGAAUCUC UUUCAACUAAUAAGAGAC AUUAUCACGAAACAAUU GGCCGCGGGUCACAGGU UCGAAUCCCGUCGUAGCCACCA	Expression in *E. coli*
ASH1 E3-51	1,771–1,821	AUGGAUAACUGAAUCUC UUUCAACUAAUAAGAGACAU UAUCACGAAACAAU	Chemical synthesis (Dharmacon)
HIV TAR-57 tRNA		GGCUACGUAGCUCAGUUGG UUAGAGCAGCGGCCGGG UCUCUCUGGUUAGACCAGAUC UGAGCCUGGGAGCUCUCUGG CUAACUAGGGAACCUGGCC GCGGGUCACAGGUUCGAA UCCCGUCGUAGCCACCA	Expression in *E. coli*

Underlined sequences correspond to the E3-118 or TAR sequences in tRNA fusion constructs. Sequences in boldface type indicate the Puf6p binding sites within the E3-118 zip-code element.

Table S4. Yeast strains used in this study

Yeast strain	Genotype
RJY4358	LOC1-GFP::HIS3MX6 YEplac181-ASH1 pRS314-Nup120-mCherry
RJY4359	LOC1-GFP::HIS3MX6 she3Δ::URA3 YEplac181-ASH1 pRS314-Nup120-mCherry